

Dielectric Spectroscopy on Dilute Blends of Polyisoprene/Polybutadiene: Effect of the Matrix Polydispersity on the Dynamics of Probe Polyisoprene

Beng Teik Poh

School of Industrial Technology, Universiti Sains Malaysia, 11800 Penang, Malaysia

Keiichiro Adachi*

Department of Macromolecular Science, Graduate School of Science, Osaka University, Toyonaka, Osaka 560, Japan

Tadao Kotaka

Toyota Technological Institute, Graduate School of Engineering, 2-12 Hisakata, Tenpaku-ku, Nagoya 468, Japan

Received February 13, 1996; Revised Manuscript Received June 13, 1996[®]

ABSTRACT: We report dielectric normal-mode relaxation of probe *cis*-polyisoprenes (PI) in dilute blends of PI and polybutadiene (PB) with broad molecular weight distributions (MWD). The PB matrixes included two binary PB blends of narrow-MWD PBs and one mixture of seven narrow-MWD PB fractions. Results were compared with our previous results on narrow-MWD PI/PB blends (*Macromolecules* **1995**, *28*, 3588) in which the double-logarithmic plot of the longest relaxation time τ of PIs against their molecular weights, M_I , conformed to a straight line with the slope varying from 2 (the Rouse behavior) to 3 (pure reptation) with increasing MW, M_B , of the matrix PBs. The plots for the broad-MWD blends also conformed to straight lines, indicating that the broad-MWD matrix is equivalent to a narrow-MWD matrix of an equivalent molecular weight M_{equiv} . However, as compared with the same weight-averaged M_B , the slopes are slightly smaller than those of the narrow-MWD blends, suggesting that the small MW matrix chains accelerate the rate of relaxation of the probe chain. The behavior cannot be explained quantitatively by the constraint-release model proposed by Graessley. We also examined the shape of the dielectric loss ϵ'' versus frequency f curve. All ϵ'' curves observed here are broader than the prediction of the Rouse and Doi–Edwards theories which predict that the slope of the $\log \epsilon''$ vs $\log f$ curve is -0.5 on the high-frequency side of the loss peak.

Introduction

In our previous paper,¹ we reported the dielectric *normal-mode* relaxation of a small amount of *cis*-polyisoprene (PI) dissolved in polybutadienes (PB) with narrow molecular weight distributions (MWD). Since PI possesses the type-A dipoles aligned in the direction parallel to the chain contour while PB does not,^{2,3} only the dynamics of PI chains can be observed in the PB matrixes of any molecular weight (MW) under different conditions of entanglement between PI and PB chains. We found that the longest relaxation time τ of PI conformed to an empirical equation given by

$$\tau \propto M_I^\alpha \quad \text{for } M_I > M_e^B \quad (1)$$

where M_I is the (weight average) MW of the PI probe and M_e^B , the MW between entanglements of PB.¹ The exponent α depended on the MW (M_B) of PB: $\alpha = 2.0$ in the range of $M_B < 3000$ but $\alpha = 3.0$ for $M_B > 20\,000$. In the intermediate range of $3000 < M_B < 20\,000$, α increased monotonously with M_B from 2 to 3 for $M_I > M_e^B$. This behavior was explained semiquantitatively with the *constraint-release* model proposed by Graessley.⁴ The exponent $\alpha = 3$ observed in high-MW matrixes was explained with the pure reptation mechanism by de Gennes^{5–7} and was first observed in dilute blends of low-MW PI probe in high-MW PI matrix.^{8,9} The exponent $\alpha = 3$ is obviously smaller than $\alpha = 3.5 \pm 0.3$ for narrow-MWD melts known as the 3.4 power law.^{10–12}

In fact the *dielectric normal-mode* relaxation time of narrow-MWD bulk PI was proportional to $M_I^{3.7}$ for $M_I > M_e^I$ ($\approx 2M_e^I$), the *characteristic* molecular weight of bulk PI.^{3,13,14} We found that the behavior of the PI/PB blends and of the bulk PI are consistent: The exponent α of the former with a constant ratio of $M_I/M_B \approx 2.5$ was 3.7 for $M_I > 5M_e^B$ ($\approx 2M_e^I$). The ratio of 2.5 is roughly the ratio of the MW between entanglements M_e^I/M_e^B of the two polymers.¹ We also found that the dielectric loss curve reflecting the distribution of relaxation times broadened with decreasing M_I/M_B as in the case of narrow-MWD PIs of condensed states with increasing M_I and/or concentrations.

The present study is an extension of the above-mentioned work to systems composed of PB matrixes with broad-MWD to understand the molecular dynamics in entangled polymers with broad-MWDs. Most of the studies reported so far on this problem were limited to narrow-MWD samples,^{15,16} and relatively few studies were concerned with the effect of MWD on the dynamics of entangled chains. Although studies on narrow distribution systems are important from a view of pure science, those on the broad-MWD systems are important as well since industrial polymeric materials have almost always broad-MWD.

To understand the relaxation behavior of a broad-MWD sample, it is needed to clarify the dynamics of each component with different MW in the sample of given MWD. For this purpose dielectric normal-mode spectroscopy is powerful because the method provides the information only of the dynamics of the chains labeled with type-A dipoles.^{2,3} In our previous study,¹

[®] Abstract published in *Advance ACS Abstracts*, August 15, 1996.

Table 1. Characteristics of PI and PB Samples

<i>cis</i> -polyisoprenes (PI) ^a			polybutadienes (PB) ^b		
code	10 ⁻³ <i>M</i> _w	<i>M</i> _w / <i>M</i> _n	code	10 ⁻³ <i>M</i> _w	<i>M</i> _w / <i>M</i> _n
PI-02	1.82		PB-02	1.8	1.04
PI-04	3.55	1.11	PB-04	4.5	1.05
PI-06	5.60	1.08	PB-05	5.1	1.04
PI-10	9.6	1.07	PB-10	10	1.05
PI-13	12.5		PB-20	20.0	1.04
PI-20	20.3		PB-33	33.0	1.05
PI-43	42.7	1.05	PB-37	37.0	1.08
PI-93	93.3		PB-63	63.0	1.08
			PB-211	211	1.08

^a The content of *cis*, *trans*, and 3,4-vinyl linkages are 83, 13.5, and 3.5%, respectively. ^b The content of *cis*, *trans*, and 3,4-vinyl linkages are 39, 52 ± 2, and 10 ± 2%, respectively.

the dynamics of PI probe in narrow-MWD PB matrix was semiquantitatively explained by Graessley's theory⁴ of constraint release which assumed that a test chain entangled with matrix chains relaxes via its own reptation and constraint release due to the motion of the matrix chains. A local jump of the test chain to a new local conformation leading to constraint release occurs when the matrix chains confining the test chain diffuse away. Then the waiting time τ_w for the local jump is proportional to the reptation time $\tau_d(M)$ of the matrix chain. For a matrix with broad-MWD (implicitly assumed all M_j 's > M_c), we may extend the Graessley theory⁴ and assume that τ_w is proportional to $1/\sum(\phi_j/\tau_d(M_j))$, where ϕ_j and M_j are the volume fraction and the MW of the j th component, respectively. The first objective of the present study is to test the Graessley's model for the dynamics of a broad-MWD system.

Recently Fodor and Hill¹⁷ studied dielectric normal mode relaxation for binary blends of PI with $M_f > M_c^i$ and concluded that the dielectric loss ϵ'' curve for the blend was given by the volume average of the ϵ'' of the components. This observation implies that the dynamics of a component chain in a broad-MWD sample is the same as that in the monodisperse sample and hence contradicts our previous observation of the dynamics of a probe PI chain being dependent on the matrix chain length.

From these points of view we have examined the mobility of probe PI chains in PB matrixes with broad-MWD. We used two binary blends of narrow-MWD PBs and a mixture of seven PB fractions as the matrixes and the MW of the probe PI was changed over a wide range.

Experimental Section

Narrow distribution samples of PI and PB were prepared through anionic polymerization in *n*-heptane at ca. 290 K with *sec*-butyllithium as the initiator. The characteristics of the samples were determined with a gel permeation chromatograph (Tosoh HLC-801A) equipped with a low-angle laser light scattering detector (Tosoh LS-8000). Details were reported in the previous paper.¹ The sample characteristics are listed in Table 1. The code number indicates the weight average MW (M_w) in kg/mol.

For preparing the matrix PB of broad-MWD, prescribed amounts of each components were dissolved in *n*-pentane to make homogeneous (ca. 5 wt % solution) and then dried in vacuum at 45 °C for 50 h. The two binary blends of PB were prepared by mixing either PB-02 or PB-05 with PB-37 at the ratio of 50/50 by weight. The blends were coded in such a way as PB-02/PB-37. The matrix of broad-MWD PB (b-PB-20) was prepared by mixing seven PB fractions among those listed in Table 1, i.e., PB-02, PB-04, PB-10, PB-20, PB-33, PB-63, and PB-211 with weight fraction w of 11.4, 17.1, 23.3, 22.1, 17.5, 7.9, and 0.7 wt %, respectively. It is noted that these three

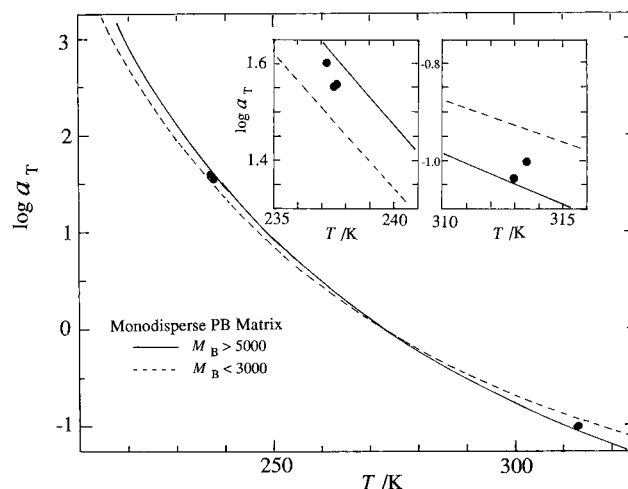


Figure 1. Temperature dependence of shift factor a_T . The solid line indicates $\log a_T$ for narrow-MWD samples of PB with molecular weight higher than 5000 and the dashed line $\log a_T$ for PB with MW = 2000.

Table 2. Characteristics of PB Matrixes

code	10 ⁻³ <i>M</i> _w	10 ⁻³ <i>M</i> _n	<i>M</i> _w / <i>M</i> _n
PB-02/PB-37	19.3	3.25	5.9
PB-05/PB-37	21.0	8.97	2.3
b-PB-20	19.9	7.21	2.8

PB matrixes have the same 10⁻³ $M_w = 20 \pm 1$ as seen in Table 2.

The blending of PI with matrix PB was made at the weight ratio of 5/95. The mixture was homogenized by dissolving it in *n*-pentane and then dried at 45 °C for 50 h.

Dielectric measurements were carried out with a transformer bridge (General Radio 1615A) in the frequency range from 30 to 15 000 Hz. Details were also reported previously.¹

Results and Discussion

Dielectric Loss Curves and Relaxation Times.

The dielectric loss maxima due to the normal mode relaxation were observed in the frequency range of 0.02 to 20 kHz at 273 K for the blends containing a PI probe with $M_w < 20 \times 10^3$. The loss peak shifted to the low-frequency side with increasing MW, and for the blends containing PI with $M_w > 43 \times 10^3$ the loss peak at 273 K went out of our experimental window. Thus to keep the loss maxima in the window, we elevated the temperature up to 390 K and constructed master curves of dielectric loss ϵ'' to cover a wide frequency range with the reference temperature 273 K. For this purpose it is needed to determine the shift factor a_T , and we utilized the previous data of a_T for the blends of PI in narrow-MWD PB matrixes¹ as follows:

Our previous data¹ indicated that the shift factor $a_T(H)$ for the blends with a high-MW matrix of $M_B > 5000$ does not depend on M_B . The constants C_1 and C_2 of the Williams-Landel-Ferry (WLF) equation¹⁰ for $a_T(H)$ are 4.69 and 138, respectively. On the other hand, C_1 and C_2 for the shift factor $a_T(L)$ for the blends with a low-MW PB matrix of $M_B \approx 2000$ and 3.95 and 130, respectively. The temperature (T) dependence of $a_T(H)$ and $a_T(L)$ are shown in Figure 1 with the solid and dashed lines, respectively.

In the present study, we used the same $a_T(H)$ for PI/(PB-05/PB-37). Since the matrixes PB-02/PB-37 and b-PB-20 contain PB-02, it is needed to determine a_T . The data points plotted in Figure 1 are a_T for PI in PB-02/PB-37 determined from the temperature dependence of the loss maximum frequency. As expected the a_T data

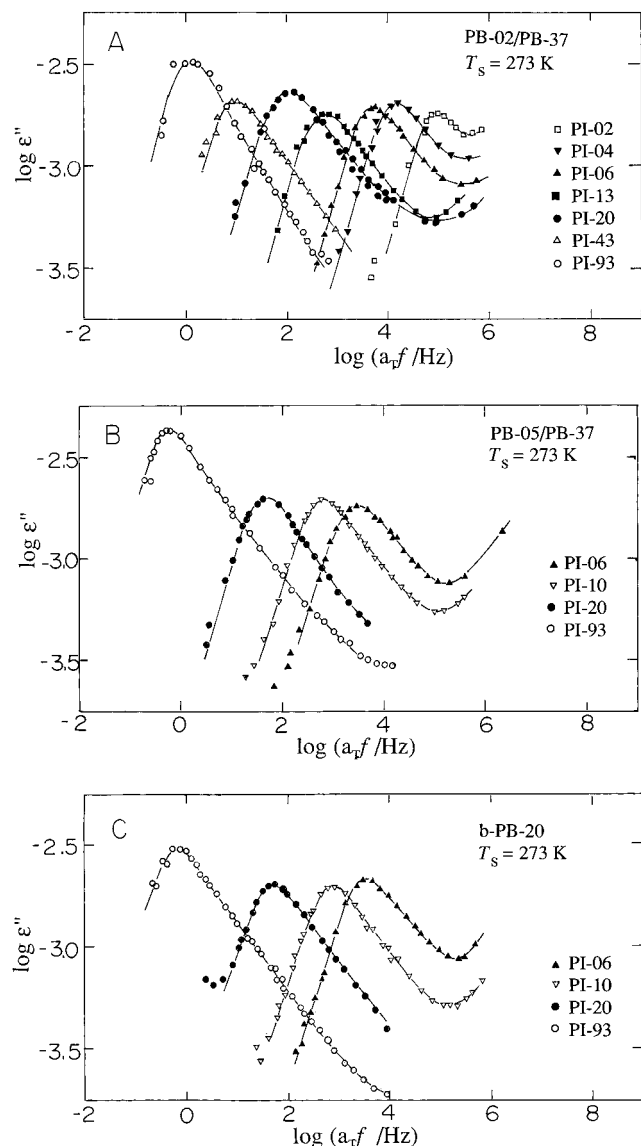


Figure 2. Master curves of $\log \epsilon''$ versus $\log f$ at 273 K. PIs dissolved in (A) PB-02/PB-37, (B) PB-05/PB-37, and (C) b-PB-20.

points locate between the solid and dashed lines. Unfortunately the plots are slightly scattered, and hence we need more data points to determine C_1 and C_2 from a set of the ϵ'' curves collected at different temperatures. To avoid this laborious task, we determined the constants by using a classic-free volume theory^{10,18} as given in the Appendix.

In the present systems $\sum \phi_i$ in eq A3 corresponds to ϕ_{02} . Thus a_T for PB-02/PB-37 is the average of the solid and dashed lines of Figure 1: $C_1 = 4.32$, $C_2 = 134$, and the standard temperature $T_0 = 273$. For the systems composed of b-PB-20 ($\phi = 0.11$) we used $C_1 = 4.61$ and $C_2 = 137$.

In this way, we constructed the master curves of ϵ'' . The double logarithmic plots of ϵ'' versus the reduced frequency $a_T f$ at 273 K for PI/(PB-02/PB-37), PI/(PB-05/PB-37), and PI/b-PB-20 are shown in Figure 2A–C, respectively. We see that the loss maxima shift to lower frequency with increasing MW (M_I) of PI indicating that the ϵ'' maxima are due to the normal mode relaxation of the probe PI chains. The gradual increase of ϵ'' above 1 MHz is due to the local segmental motion of PB and PI.

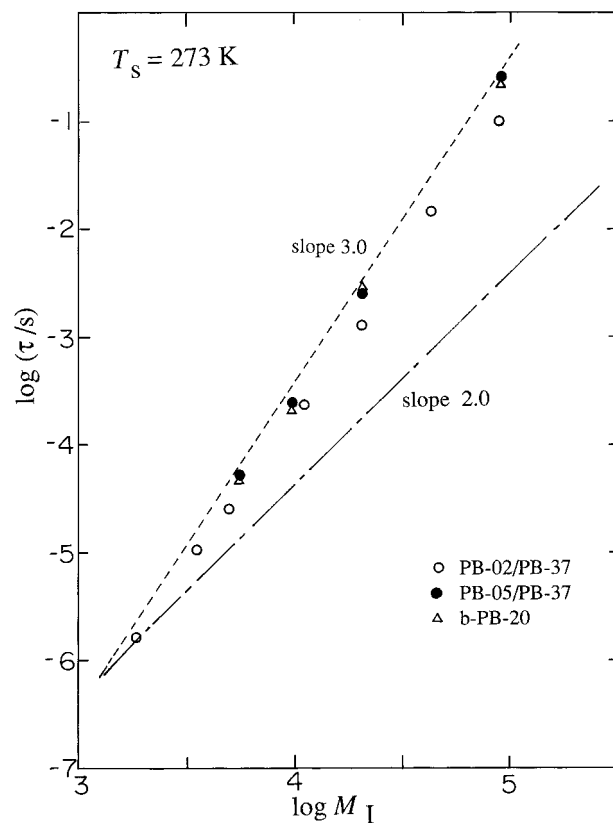


Figure 3. Double-logarithmic plot of the longest relaxation time τ versus molecular weight M_I of PI in the matrixes of broad-MWD PB. The dashed line and dash-dot line indicate the $\log \tau$ versus $\log M_I$ for narrow-MWD PB with $M_B \geq 20\,000$ and $M_B = 2000$, respectively.

As we pointed out frequently in our previous papers,^{1,3} the longest relaxation time τ is given from the loss maximum frequency f_m for linear type-A chains:

$$\tau = 1/(2\pi f_m) \quad (2)$$

Figure 3 shows the double logarithmic plot of τ versus M_I . The dashed line indicates the data on τ in narrow-MWD PBs, i.e., the slope 3.0 was observed for the case of $M_B \geq 20\,000$. On the other hand, the dash-dot line with the slope 2.0 is for $M_B = 2000$.¹ It is seen that τ , for the present system, falls between these two lines. The plots are almost straight as observed for the blends of PI/narrow-MWD PBs. However, carefully examining the slopes, we find that the slope is somewhat smaller for the present broad-MWD system than for the previous narrow-MWD blends, presumably reflecting the situation that the low-MW component accelerates the constraint release.

Relaxation Time in an Isofriction State. For the quantitative discussion on the M_I dependence of τ ,^{10,11} we need to reduce the τ data to an isofriction state. Using eq A3, we reduced the friction coefficients ζ in PB-02/PB-37 and b-PB-20 matrixes to that in the high-MW PB matrixes and determined the *isofriction state* relaxation time τ_ζ . In our previous paper,¹ we estimated that $\log \zeta(H) - \log \zeta(L) = 0.176$. Thus $\log \zeta$ of PB-02/PB-37 was reduced by 0.084 and that of b-PB-20 by 0.02. For the matrix of PB-05/PB-37, the correction was not necessary. Figure 4 shows the *isofriction state* relaxation times τ_ζ thus obtained.

We see that the $\log \tau_\zeta$ versus M_I curves conform to straight lines and converge to the point at which $\log \tau_\zeta = -5.5$ and $\log M_I = 3.3$ ($M_I \approx 2000$). Similar behavior

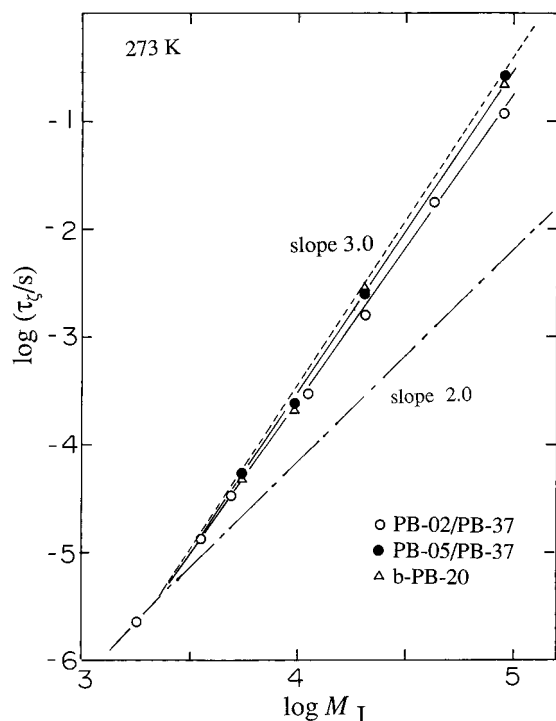


Figure 4. Double-logarithmic plot of the longest relaxation time τ_z reduced to an isofriction state against molecular weight M_I of PI in the matrices of broad-MWD PB. The dashed line and dash-dot line indicate the $\log \tau_z$ versus $\log M_I$ for narrow-MWD PB with $M_B \geq 20\,000$ and $M_B = 2000$, respectively.

was observed for PI/narrow-MWD PBs.¹ The slopes α of the straight lines for the matrixes of PB-02/PB-37, PB-05/PB-37, and b-PB-20 are 2.75, 2.91, and 2.91, respectively. These slopes are smaller than the slope 3.0 for the blend of PI/narrow-MWD PB with $M_w = 20\,000$.¹ In fact the slope becomes smaller with increasing content of PB-02 in the matrix even when weight average M_B 's are the same.

We also see that as far as the MI dependence of τ is concerned, the behavior in the matrixes with broad distribution of MW is the same as those in the narrow-MWD matrixes. Therefore we define an equivalent molecular weight M_{equiv} for a broad-MWD PB as the MW of monodisperse PB matrix having the same α . From our previous data of α ,¹ the values of M_{equiv} for PB-02/PB-37, b-PB-20, and PB-05/PB-37 were determined to be 10 600, 15 000, and 15 000, respectively. (Compare with the true M_w listed in Table 2.)

To discuss the meaning of M_{equiv} , we compare the observed MI dependences of τ with that predicted by the original tube model proposed by de Gennes⁵ and developed by Doi and Edwards.^{6,7} We consider three systems in which a trace amount of a guest chain with MW = M_g is dissolved (a) in a monodisperse matrix with MW = M_m or in two types of 50/50 blends of matrix chains with MW = M_m (1) and M_m (2). One is the case (b) where M_m (1) < M_e < M_m (2) and the other (c) is M_e < M_m (1) < M_m (2). For simplicity we assume the guest chain and the matrix chain are chemically the same.

In Figure 5, the M_g dependence of τ is schematically depicted. The dash-dot line (the M^3 dependent) and dotted line (M^2 dependent) indicate, respectively, τ in a monodisperse matrix with $M_m = \infty$ and with $M_m < M_e$. For simplicity, we assumed that the dash-dot and dotted lines cross at M_e as observed in our earlier study on monodisperse PI/PI blends.¹ We have neglected the front factor 3 in the expression of $\tau = 3\tau_R(M_g/M_e)^3$ in

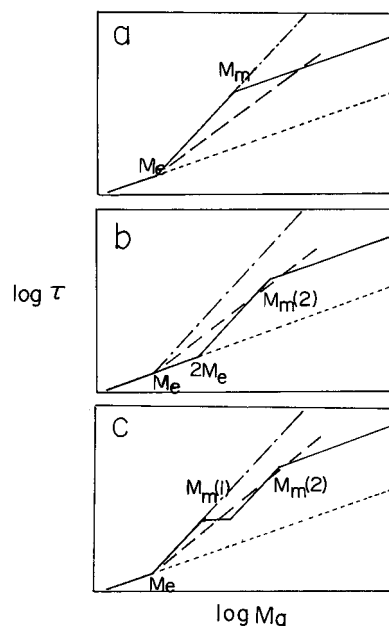


Figure 5. Schematic diagrams of the dependence of the longest relaxation time τ of a guest chain on its MW M_g in matrixes of (a) monodisperse matrix with MW = M_m and binary 50/50 blends of chains with MW = M_m (1) and M_m (2); (b) the case M_m (1) < M_e < M_m (2) and (c) M_e < M_m (1) < M_m (2).

the Doi-Edwards theory, where τ_R is the Rouse relaxation time at MW = M_e .^{7,19}

We consider the case (a) in which the matrix is monodisperse. When $M_e < M_g < M_m$, the slope α is predicted to be 3.0 (the dash-dot line), but when $M_e < M_m < M_g$, the matrix chains eventually act as a solvent and the guest chain behaves as a Rouse chain with the slope of 2.0 as shown schematically with the solid line in Figure 5A. On the other hand the experimental plot conforms to the dashed line as reported previously.¹

Next we consider the behavior of the case (b) corresponding to PI(PB-02/PB-37). The component with MW = M_m (1) acts as a solvent in the system and M_e increases twice as high as that in monodisperse matrix as M_e is proportional to the inverse of the polymer concentration (here $\phi = 0.5$).¹⁰ Thus for the system in which $2M_e < M_g < M_m$ (2), the τ vs M_g curve has the slope 3.0. In the range of M_m (2) < M_g , the slope becomes 2.0 as shown schematically in Figure 5b. However, the experimental τ_z curve exhibited the slope of 2.75 as mentioned above. This behavior is represented by the dashed line in Figure 5.

Case (c) corresponds to the PI(PB-05/PB-37) system. Similar considerations to the case (b) result in the curve shown in Figure 5c. There exist three different regimes for the motion of the guest chains. On the other hand, the present experimental results did not exhibit such a fine structure as shown in Figure 5c by the dashed line.

From these results we see that all structures in the double-logarithmic plot of τ vs M_g predicted by the original tube model are completely smeared out by mechanisms other than reptation. In our previous study we concluded that the constraint release model by Graessley is most likely this unknown mechanism. Thus we expect that a PB matrix with a certain constraint release time becomes equivalent to the monodisperse PB having the same constraint release time as the broad-MWD PB. These considerations support the existence of M_{equiv} for broad-MWD systems.

In the PI/broad distribution PB systems, the tube dilation and the constraint release occur continuously with increasing MW of the probe PI. Thus the PI/b-PB-20 also exhibits straight $\log \tau$ versus $\log M_f$ curve.

As mentioned above, the dynamics of PI in the matrix of PB-02 conformed well to the Rouse theory.¹⁹ Therefore, one may expect that PB-02 acts as a solvent in the PI/(PB-02/PB-37) system. However, the experimental τ_c curve exhibited the slope of 2.75 as shown in Figure 4. This suggests that PB-02 does not act as an ordinary solvent, but it still contributes somehow to the entanglement. In fact the M_e of PB was estimated to be 1900 and is close to the MW of PB-02 with $M_w = 1800$.

Comparison with the Constraint Release Model. We consider the matrix composed of chains with molecular weight $M_1, M_2, \dots, M_j, \dots, M_n$. The volume fractions of the j th component is ϕ_j and these chains form a tube around a test chain. The Graessley theory⁴ assumes that there are z gates for local conformational jump of the tube. The probability that a certain gate is occupied by the j th chain may be proportional to ϕ_j . Then the waiting time τ_w for the local jump is given by

$$\tau_w = \int_0^\infty \prod_{j=1}^n [(8/\pi^2) \sum_{p:\text{odd}} (1/p^2) \exp\{-tp^2/\tau_d(M_j)\}]^{z\phi_j} dt \quad (3)$$

where p is the mode number and $\tau_d(M_j)$ the reptation time of the j th component being proportional to M_j^3 . If the higher modes of $p \geq 3$ are neglected, τ_w is given by

$$\tau_w = 1/[z \sum \phi_j / \tau_d(j)] \quad (4)$$

Then the tube moves as if it were a Rouse chain with the characteristic time $\tau_{cr} = (2/\pi^2)(M_g/M_e)^2 \tau_w$. These equations predict that a matrix composed of more than two components can be replaced by an equivalent monodisperse matrix with M_{equiv} satisfying

$$M_{equiv} = (1/\sum \phi_j / M_j^3)^{1/3} \quad (5)$$

The values of M_{equiv} for PB-05/PB-37 and b-PB-20 are calculated to be 6400 and 7500, respectively. In the calculation for b-PB-20, we assumed that PB-02 is in the Rouse regime and does not contribute to the entanglement effect. If we take into account PB-02 in the calculation of eq 5, we obtain $M_{equiv} = 3800$. For PB-02/PB-37 we did not calculate M_{equiv} because PB-02 is close to the Rouse regime. These theoretical values of M_{equiv} do not agree with the experimental M_{equiv} given in the previous section. The reason for the disagreement may be the assumption that the surrounding chains around the test chain move by the pure reptation mechanism. In the matrixes with broad-MWD, the dynamics of the matrix chain is greatly modified from the pure reptation mechanism, and hence eq 5 does not give a correct waiting time.

Then the problem is what average MW may correspond to M_{equiv} in a polydisperse system. We sought an empirical equation to represent M_{equiv} . As is seen in Table 2, both M_w and M_n do not agree with the observed M_{equiv} . It appears that high-MW components do not contribute much to M_{equiv} . Therefore we may assume that the components with $M > 20\,000$ are equivalent to the component with $M = 20\,000$ and then calculate weight average MW to be 11 000, 12 500, and 13 100, respectively, for PB-02/PB-37, PB-05/PB-37, and

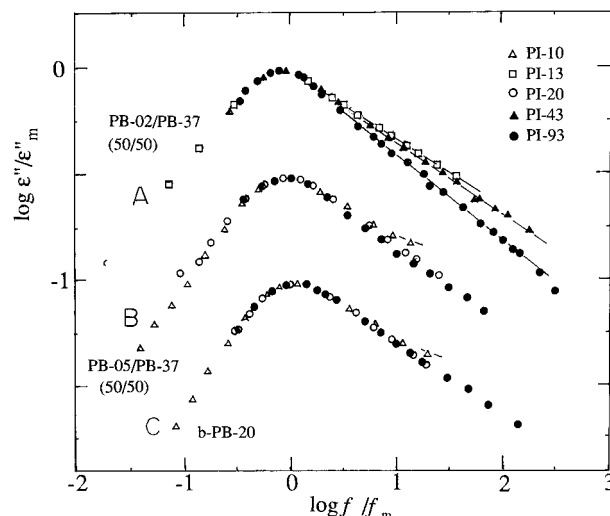


Figure 6. Plot of dielectric loss ϵ'' divided by the maximum value ϵ''_m of loss against f/f_m .

b-PB-20. These values are comparable to the observed M_{equiv} but slightly smaller than the observed M_{equiv} .

Shape of Loss Curves. Figure 6 shows the normalized ϵ'' curves of PIs with different MW in the three PB matrixes used in this study, i.e., the curves of groups A, B, and C are those in PB-02/PB-37, PB-05/PB-37, and b-PB-20, respectively. In A, we see that the ϵ'' curves broaden with decreasing MW of PI. Such a behavior was observed previously for PIs in narrow-distribution PBs. The negative slopes κ of the $\log \epsilon''$ curve on the high-frequency side can be a measure of the broadness of the ϵ'' curve and are 0.35, 0.36, and 0.41 for PI-13, PI-43, and PI-84, respectively. Here we did not determine κ for PI-20 since data points are rather scattered. For PB-05/PB-37 and b-PB-20 matrixes, κ is 0.36 irrespective of the MW of PI.

In our previous paper²⁰ on the dielectric relaxation of PI in semidilute solution, we reported that the slope κ was ca. 0.65 in dilute solutions in accord with the Zimm theory²¹ ($\kappa = 2/3$) but κ decreased with increasing polymer concentration and saturated to a value of ca. 0.30 around C which is 10 times higher than the overlapping concentration (ca. 3 wt % for PI-140). If we assume that PB-02 acts as a solvent in PB-02/PB-37, the blend is 50% solution of PB-37, and hence we expect that in the present PB matrixes, the value of κ is ca. 0.3. However, contrary to our expectation, $\kappa = 0.41$, which is larger than 0.3 for PI-84 in PB-02/PB-37. This result indicates that the slope is a complex function of concentration and relative MW of the guest and matrix chains.

Finally we examine the relationship between κ and M_{equiv} . The value of M_{equiv} of PB-02/PB-37 has been given to be 10 600. In the previous study we observed $\kappa = 0.41$ for PI-86 in narrow-MWD PB with MW = 10700. This value agrees with the present result: $\kappa = 0.41$ for PI-84 in PB-02/PB-37 matrix. Thus M_{equiv} seems to govern the distribution of relaxation times as well as the MW dependence of τ .

Conclusions

The double-logarithmic plot of the longest relaxation time τ_c of an isofriction state against molecular weight M_f of PI in broad-distribution PB matrixes conforms to a straight line with slope α similar to that in narrow-distribution PBs. Thus there exists an equivalent narrow-MWD PB in which the slope α is the same as

the broad distribution PB. The molecular weight M_{equiv} of the narrow-MWD PB is lower than the weight-average MW of the broad distribution PB.

The experimental M_{equiv} does not agree with the theoretical M_{equiv} calculated with the constraint release model proposed by Graessley. Therefore, the slope α of the $\log \tau_\zeta$ versus $\log M_i$ in the broad-MWD matrixes cannot be explained quantitatively by the Graessley model.

Distribution of relaxation times decreased with increasing molecular weight of PI in PB-02/PB-37. The slopes κ of the $\log \epsilon''$ curve on the high-frequency side can be a measure of the broadness of the ϵ'' curve and are 0.35, 0.36, and 0.41 for PI-13, PI-43, and PI-84, respectively. On the other hand, in PB-05/PB-37 and b-PB-20 matrixes, the value of κ was 0.36 irrespective of the MW of PI.

Acknowledgment. This work was partly supported by the Ministry of Education, Science and Culture, Japan under a Grant-in-Aid for Scientific Research (06555205, 1994-1995). B.T.P. wishes to thank the University of Science, Malaysia for financial support during the period of this research program.

Appendix

We consider the monomeric friction coefficient ζ of a guest PI chain in PB blends. Classical free-volume theory gives ζ by the form¹⁸

$$\log \zeta = 1/\psi + K \quad (\text{A1})$$

where ψ is the free-volume fraction of the system and K is a constant. We can split ψ into the free-volume fraction ψ_0 independent of MW and that ψ_{end} created by the chain ends which are inversely proportional to the number-average MW, M_n . Then we may rewrite eq A1 as

$$\log \zeta = 1/(\psi_0 + \psi_{\text{end}}) + K \quad (\text{A2})$$

Thus ψ decreases slightly with increasing MW and reaches ψ_0 . For narrow-MWD PB, ψ is independent of

MW for MB > 5000. For a broad-MWD matrix, ψ_{end} is proportional to $\sum \phi_j/M_{nj}$, where ϕ_j and M_{nj} are the volume fraction and the number-average MW of the j th component. Obviously $\psi_0 \gg \psi_{\text{end}}$, as long as the MW of the components is not extremely low, and then $\log \zeta$ of a binary blend composed of a high-MW component H and a low-MW component L is approximately given by

$$(\log \zeta_H - \log \zeta)/(\log \zeta_H - \log \zeta_L) \approx \phi_L \quad (\text{A3})$$

where ζ_H and ζ_L are the friction coefficients of the H and L components, respectively, and ϕ_L is the volume fraction of the L component.

References and Notes

- (1) Adachi, K.; Wada, T.; Kawamoto, T.; Kotaka, T. *Macromolecules* **1995**, *28*, 3588.
- (2) Stockmayer, W. H. *Pure Appl. Chem.* **1967**, *15*, 539.
- (3) Adachi, K.; Kotaka, T. *Prog. Polym. Sci.* **1993**, *18*, 585.
- (4) Graessley, W. W. *Adv. Polym. Sci.* **1982**, *47*, 68.
- (5) De Gennes, P.-G. *J. Chem. Phys.* **1971**, *55*, 572.
- (6) Doi, M.; Edwards, S. F. *J. Chem. Soc., Faraday Trans. 2*, **1978**, *74*, 1789, 1802, 1818.
- (7) Doi, M.; Edwards, S. F. *Theory of Polymer Dynamics*; Clarendon Press: Oxford, 1986.
- (8) Adachi, K.; Nishi, I.; Itoh, S.; Kotaka, T. *Macromolecules* **1990**, *23*, 2550.
- (9) Adachi, K.; Itoh, S.; Nishi, I.; Kotaka, T. *Ibid.* **1990**, *23*, 2554.
- (10) Adachi, K.; Nakamoto, T.; Kotaka, T. *Macromolecules* **1989**, *22*, 3111. Adachi, K.; Kotaka, T. *J. Non-Cryst. Solids* **1991**.
- (11) Ferry, J. D. *Viscoelastic Properties of Polymers*, 3rd ed.; John Wiley: New York, 1980.
- (12) Graessley, W. W. *Adv. Polym. Sci.* **1974**, *16*, 1.
- (13) Berry, G. C.; Fox, T. G. *Adv. Polym. Sci.* **1968**, *5*, 261.
- (14) Imanishi, Y.; Adachi, K.; Kotaka, T. *J. Chem. Phys.* **1988**, *89*, 7585.
- (15) Boese, D.; Kremer, F. *Macromolecules* **1990**, *23*, 829; *131-133*, 723.
- (16) Watanabe, H.; Kotaka, T. *Macromolecules*, **1987**, *20*, 535.
- (17) Zawada, J. A.; Fuller, G. G.; Colby, R. H.; Fetters, L. J.; Roovers, J. *Macromolecules* **1994**, *27*, 6851.
- (18) Fodor, J. S.; Hill, D. A. *Macromolecules* **1993**, *26*, 5379.
- (19) Doolittle, A. K. *J. Appl. Phys.* **1951**, *22*, 1471.
- (20) Rouse, P. E. *J. Chem. Phys.* **1953**, *21*, 1272.
- (21) Urakawa, O.; Adachi, K.; Kotaka, T. *Macromolecules* **1993**, *26*, 2036-2042.
- (22) Zimm, B. H. *J. Chem. Phys.* **1956**, *24*, 269.

MA960222A